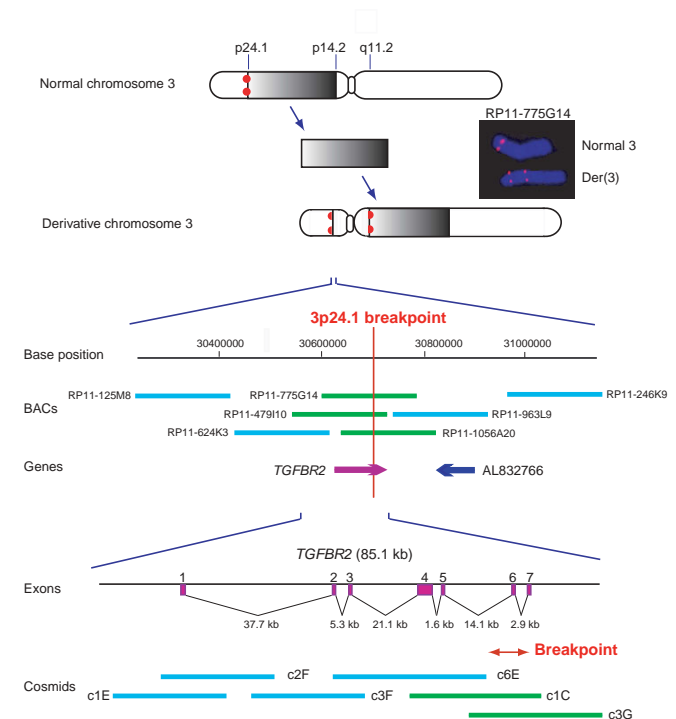


## Heterozygous *TGFBR2* mutations in Marfan syndrome

Takeshi Mizuguchi<sup>1,2,16</sup>, Gwenaëlle Collod-Beroud<sup>3,4,16</sup>, Takushi Akiyama<sup>5</sup>, Marianne Abifadel<sup>4</sup>, Naoki Harada<sup>1,2,6</sup>, Takayuki Morisaki<sup>7</sup>, Delphine Allard<sup>4</sup>, Mathilde Varret<sup>4</sup>, Mireille Claustres<sup>3</sup>, Hiroko Morisaki<sup>7</sup>, Makoto Ihara<sup>8</sup>, Akira Kinoshita<sup>1,2</sup>, Koh-ichiro Yoshiura<sup>1,2</sup>, Claudine Junien<sup>4,9</sup>, Tadashi Kajii<sup>10</sup>, Guillaume Jondeau<sup>4,11</sup>, Tohru Ohta<sup>2,12,13</sup>, Tatsuya Kishino<sup>2,12</sup>, Yoichi Furukawa<sup>14</sup>, Yusuke Nakamura<sup>14</sup>, Norio Niikawa<sup>1,2</sup>, Catherine Boileau<sup>4,9,16</sup> & Naomichi Matsumoto<sup>1,2,15,16</sup>

Marfan syndrome is an extracellular matrix disorder with cardinal manifestations in the eye, skeleton and cardiovascular systems associated with defects in the gene encoding fibrillin (*FBN1*) at 15q21.1 (ref. 1). A second type of the disorder (Marfan syndrome type 2; OMIM 154705) is associated with a second locus, *MFS2*, at 3p25–p24.2 in a large French family (family MS1)<sup>2</sup>. Identification of a 3p24.1 chromosomal breakpoint disrupting the gene encoding TGF- $\beta$  receptor 2 (*TGFBR2*) in a Japanese individual with Marfan syndrome led us to consider *TGFBR2* as the gene underlying association with Marfan syndrome at the *MFS2* locus. The mutation 1524G→A in *TGFBR2* (causing the synonymous amino acid substitution Q508Q) resulted in abnormal splicing and segregated with *MFS2* in family MS1. We identified three other missense mutations in four unrelated probands, which led to loss of function of TGF- $\beta$  signaling activity on extracellular matrix

formation. These results show that heterozygous mutations in *TGFBR2*, a putative tumor-suppressor gene implicated in several malignancies, are also associated with inherited connective-tissue disorders.



**Figure 1** *TGFBR2* was isolated from the 3p24.1 breakpoint of a Japanese individual with complex chromosomal abnormalities. The 3p24.1 breakpoint was analyzed because the *MFS2* locus was also mapped to 3p25–p24.2. In this individual, the chromosomal segment 3p24.1–p14.2 was inserted into 3q11.2. FISH analysis confirmed that RP11-775G14 spans the 3p24.1 breakpoint. A summarized physical map covering the 3p24.1 breakpoint is indicated. Horizontal bars show BAC and cosmid clones; green depicts clone spanning the breakpoint; and the arrow shows the gene. *TGFBR2* exons are indicated as purple squares. Cosmid subclones c1C and c3G spanned the breakpoint. c1C contains 35.2 kb of the genomic region of *TGFBR2* (from intron 3 to the end of 3' untranslated region) out of the 39.4 kb of insert DNA, according to its end sequence information. The gene must have been disrupted at the breakpoint because signals on the 3q would have not been seen if the breakpoint existed outside *TGFBR2*.

<sup>1</sup>Department of Human Genetics, Nagasaki University Graduate School of Biomedical Sciences, Nagasaki Japan. <sup>2</sup>CREST, Japan Science and Technology Agency, Kawaguchi, Japan. <sup>3</sup>Laboratoire de Génétique Moléculaire, Institut Universitaire de Recherche Clinique, Montpellier, France. <sup>4</sup>INSERM U383, Université Paris V, Hôpital Necker-Enfants Malades, Paris, France. <sup>5</sup>Division of Pediatric Surgery, National Okayama Medical Center, Okayama, Japan. <sup>6</sup>Kyushu Medical Science Nagasaki Laboratory, Nagasaki, Japan. <sup>7</sup>Department of Bioscience, National Cardiovascular Center Research Institute, Suita, Japan. <sup>8</sup>Department of Radiation Biophysics, Nagasaki University Graduate School of Biomedical Sciences, Nagasaki, Japan. <sup>9</sup>Laboratoire de Biochimie, d'Endocrinologie et de Génétique Moléculaire, Hôpital Ambroise Paré, Boulogne, France. <sup>10</sup>Hachioji, Japan. <sup>11</sup>Service de Cardiologie, Hôpital Ambroise Paré, Boulogne, France. <sup>12</sup>Division of Functional Genomics, Center for Frontier Life Sciences, Nagasaki University, Nagasaki, Japan. <sup>13</sup>The Research Institute of Personalized Health Sciences, Health Sciences University of Hokkaido, Ishikari-tobetsu, Japan. <sup>14</sup>Human Genome Center, Institute of Medical Science, The University of Tokyo, Tokyo, Japan. <sup>15</sup>Department of Human Genetics, Yokohama City University Graduate School of Medicine, Yokohama, Japan. <sup>16</sup>These authors equally contributed to this work. Correspondence should be addressed to N.M. (naomat@yokohama-cu.ac.jp) or C.B. (boileau@necker.fr).

We encountered a Japanese individual with Marfan syndrome with *de novo* complex chromosomal rearrangements, 46,XY,t(1;5;4)(p35;q33.2;q35),ins(3)(q11.2;p24.1p14.2). As one of these chromosomal breakpoints, 3p24.1, was consistent with the *MFS2* locus and the individual carried no mutations in *FBN1* (data not shown), we investigated whether disruption of a gene at 3p24.1 by the insertion caused the disease. Fluorescence *in situ* hybridization (FISH) mapping showed that BAC clones, RP11-479I10, RP11-775G14 and RP11-1056A20, spanned the breakpoint (Fig. 1). Only the gene *TGFBR2* was in the common region overlapped by the three BACs and was disrupted at the breakpoint, according to detailed FISH analysis using cosmid subclones derived from RP11-775G14 (Fig. 1).

We analyzed *TGFBR2* in a large French family (family MS1) in whom we mapped *MFS2* at 3p25–p24.2 (ref. 2; Fig. 2a) and found the nucleotide substitution 1524G→A in all of the three affected individuals that we initially tested. This transition is synonymous (amino acid substitution Q508Q) but is located at the last nucleotide of exon 6, implying that a splicing process could be affected. RT-PCR analysis with a primer set in exons 5 and 7 using cDNA of fibroblasts from two affected family members (individuals III-37 and IV-10) identified a stable, larger product along with the expected normal band (Supplementary Methods online). Sequencing analysis confirmed an abnormal splicing, by which 23 nucleotides of intron 6 were added to

exon 6, creating a premature stop codon at amino acid position 525 (Fig. 2b). Quantitative experiments showed that the two forms were expressed equally (Supplementary Methods online). We did not detect the abnormal fragment in fibroblast cDNA from individual III-41 (healthy) or from an unrelated normal control.

We then analyzed samples from all 74 members of family MS1 by PCR and direct sequencing of exon 5 using genomic DNA as a template. We detected the 1524G→A substitution in 25 members (12 affected individuals and 13 with an ambiguous status) but not in 32 healthy siblings, one individual with an ambiguous status (individual IV-53) and 16 unrelated spouses. The substitution was also absent in 60 French, 92 independent CEPH and 267 Japanese healthy controls. Molecular data for members of family MS1 were consistent with clinical data, except for one subject (individual IV-53; ref. 3). This ‘ambiguous’ individual presented with skeletal features and an aortic diameter of 32 mm (+1.98 s.d.) at age 16 (ref. 3). He is now 32 years old, has a normal aortic diameter and should be considered unaffected. Carriers of the 1524G→A mutation shared the common haplotype at *D3S1609*, *D3S3727* (intragenic *TGFBR2* marker), *D3S3567* and *D3S1619* (Fig. 2a).

We then studied nine Marfan syndrome probands from nine unrelated French families and ten unrelated Japanese individuals with Marfan syndrome who had no mutations in or linkage to

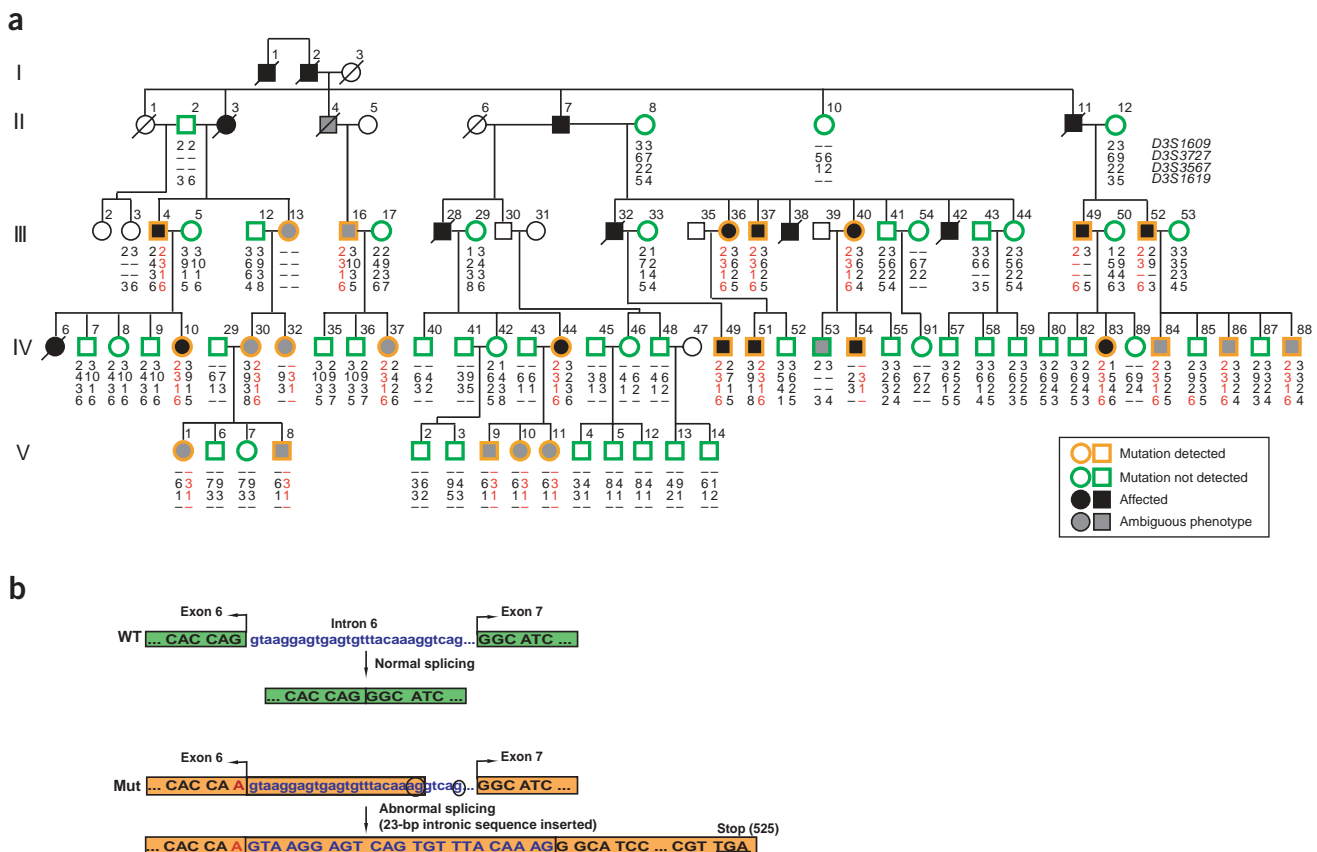


**Figure 2** Haplotype analysis of a large French family (family MS1) and a mutation causing abnormal splicing. **(a)** Pedigree of family MS1 and segregation of 3p24.1 markers in members affected with Marfan syndrome (black symbols), having an ambiguous status (gray symbols) or unaffected (white symbols). Orange symbols indicate members with the mutation 1524G→A, and green symbols members without the mutation. The haplotype cosegregating with the disease is shown in red. **(b)** Normal (green) and abnormal splicing (orange) caused by 1524G→A. The consensus value on splicing<sup>22</sup> was modified from 95.6 to 82.3 by 1524G→A, and another good consensus sequence (AGgt xgg, value 90.5) was located 23 bp away in the intronic sequence. In the mutated allele, 23 nucleotides of intron 6 were newly added after exon 6 and connected to regular exon 7 as predicted, resulting in a premature stop codon at amino acid 525. WT, wild-type; Mut, mutated.

*FBN1*. Using bidirectional sequencing of all seven exons of *TGFBR2*, we identified three missense mutations: 923T→C (resulting in the amino acid substitution L308P), 1346C→T (resulting in the amino acid substitution S449F) and 1609C→T (resulting in the amino acid substitution R537C). Mutation 923T→C was found only in the proband of French family MS57 but not in her unaffected parents (paternity confirmed) or in two healthy siblings, indicating that the mutation occurred *de novo*. Mutation 1346C→T was identified in a French family (family MS382), and mutation 1609C→T in another French family (family MS587) and in one Japanese individual. In family MS587, the proband (individual III-7) and two affected members (individuals III-1 and IV-1), as well as a child with an ambiguous status (individual IV-3), carried mutation 1609C→T (Fig. 3). All the missense mutations are located in the serine-threonine kinase domain of TGF-β receptor 2, and each affects an amino acid that is highly conserved or chemically similar in the proteins encoded by the homologous mouse and rat *Tgfr2*, mouse and zebrafish *Acrv2* and nematode *daf* proteins (Fig. 3). We did not find the mutations in 267 unrelated Japanese (534 chromosomes) or 92 independent CEPH healthy controls (184 chromosomes). We also investigated 10 French probands with thoracic aortic aneurysms and dissection (TAAD), because a locus with putative associated with this disease has been mapped at 3p25–24 (ref. 4), but identified no mutations.

We used an *in vitro* luciferase assay to evaluate the effect of the mutations on TGF-β signaling. We transfected a pTARE-Luc *cis*-reporter plasmid and a pRL-TK vector into HEK 293 cells and determined relative luciferase activity (RLA). We detected basal activity that increased threefold after exposure to exogenous TGF-β1 (Fig. 4a). Transfection with wild-type *TGFBR2* cDNA resulted in RLA of 15 even in the absence of exogenous TGF-β1 (RLA of ~12) as previously reported<sup>5</sup>. In contrast, RLA decreased significantly in the truncated mutant δ cyt, lacking the kinase domain, even with exogenous TGF-β1. Transfection with the other missense mutants, L308P, S449F and R537C, also caused significant decreases in RLA, indicative of their negative effect on TGF-β signaling.

TGF-βs are cytokines that regulate many cellular processes, including proliferation, cell cycle arrest, apoptosis, differentiation and extracellular matrix formation, through a heteromeric complex of type I and type II receptors with serine-threonine kinase activities in their cytoplasmic domains. Defective TGF-β signal transduction is important in tumorigenesis, and *TGFBR2*, *SMAD4* and *SMAD2* act as tumor suppressors in several cancers<sup>6</sup>. Most mutations in *TGFBR2* found in tumor cells are clustered in the poly-A repeat in exon 3 (ref. 7; Fig. 3). Many missense mutations in *TGFBR2* are associated with various cancers and have been suggested to result in loss of function<sup>5,8–10</sup>. Only one germline mutation (944C→T, resulting in the amino acid substitution T315M, located

in the kinase subdomain IV of the receptor) has been reported in a kindred with hereditary nonpolyposis colorectal cancer<sup>11</sup>.

As we analyzed *TGFBR2* in different populations, we found that 7 of 492 normal Japanese controls (0.71% allele frequency) and 6 of 228 individuals with sporadic colorectal cancer (1.32%) were heterozygous with respect to mutation 944C→T. As the frequency in the two populations was not statistically different ( $P > 0.05$  by  $\chi^2$  analysis), 944C→T could in fact be a rare polymorphism. Functional studies<sup>12</sup> indicated that T315M mutant protein had a defect in growth inhibition in response to TGF-β but maintained the ability to induce extracellular matrix proteins, suggesting that two divergent TGF-β signaling transduction pathways may exist. Experiments using the p3TP-Lux reporter system and *Tgfr2*-negative DR-26 cells showed that the three missense mutations found in Marfan syndrome suppressed RLA markedly, suggesting that an extracellular matrix protein, plasminogen activator inhibitor type 1 (PAI-1), was downregulated in Marfan syndrome (Fig. 4b). The T315M missense mutation reported in hereditary nonpolyposis colorectal cancer<sup>12</sup> did not suppress RLA of p3TP-Lux. These diverging effects of the different mutations may explain why malignancies were not observed in families with Marfan syndrome with the *TGFBR2* mutations. Furthermore, cotransfection of DR-26 cells with different ratios of wild-type and R537C TGF-β protein (25:75, 50:50 and 75:25) caused a progressive increase of RLA in parallel with the quantity of wild-type cDNA, suggesting that the

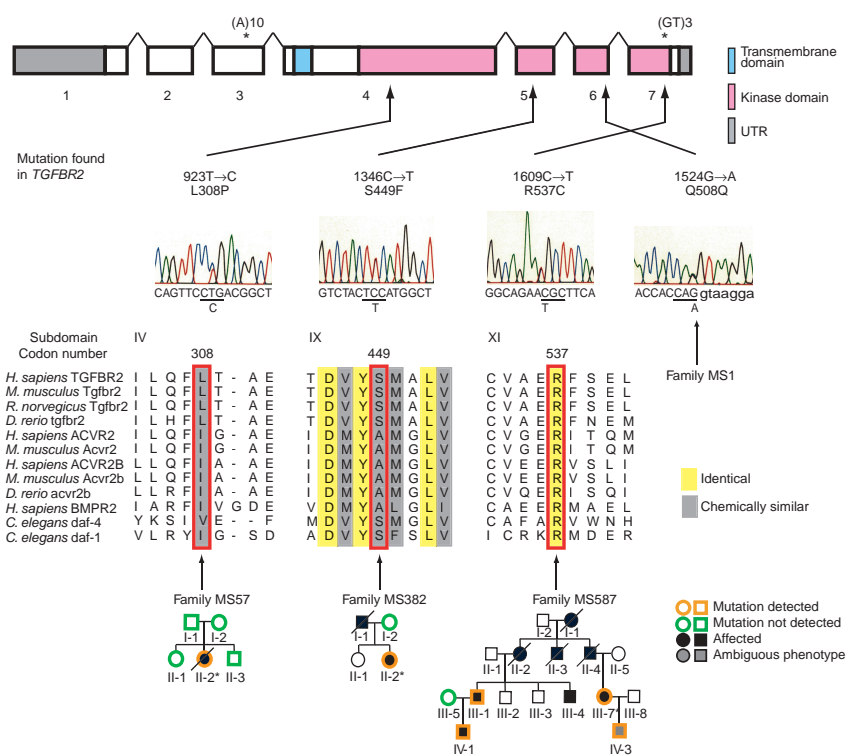


**Figure 3** Genomic structure of *TGFBR2* and mutations found in families with Marfan syndrome. *TGFBR2* consists of seven exons (squares). A transmembrane domain, a kinase domain and the untranslated regions are shown in light blue, pink and gray, respectively. (A)10 and (GT)3 are genomic instability sites. Three other missense mutations, 923T→C, 1346C→T and 1609C→T are found in families MS57, MS382 and MS587, respectively. Symbols (filled, open, green and orange) are as described for Figure 2. Asterisks indicate the proband in each family. Each mutation occurred at an amino acid that is evolutionarily conserved or chemically similar (red square) in a kinase domain among mouse and rat *Tgfr2*, mouse and zebrafish *Acrv2*, and nematode *daf* proteins. Multiple sequence alignment was done using CLUSTALW.

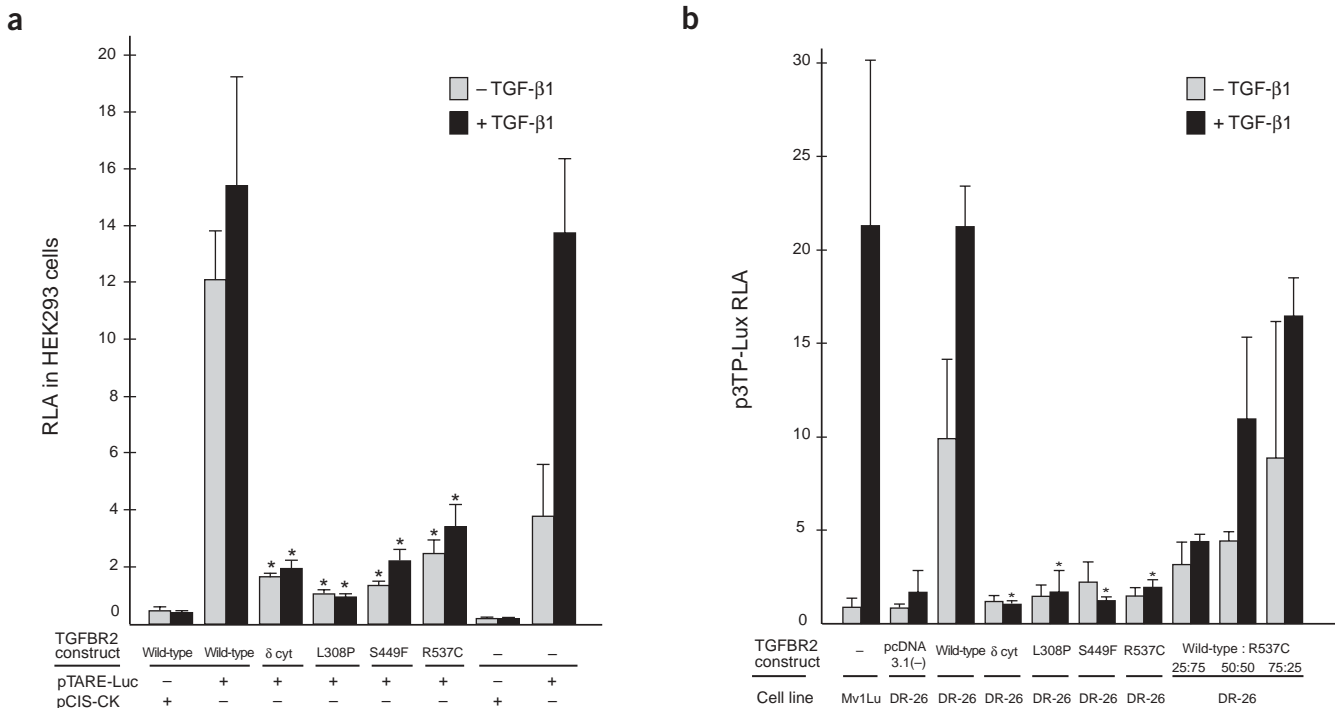


**Figure 4** Impairment of TGF- $\beta$  signaling activity by *TGFBR2* missense mutations in individuals with Marfan syndrome. **(a)** RLA of pTARE-Luc *cis*-reporter in HEK 293 cells after transient transfection with various *TGFBR2* constructs was calculated by normalization using the activity of a cotransfected control vector, pRL-TK, containing distinguishable *R. reniformis* luciferase. Data represent mean + s.d. Basal activity only by pTARE-Luc *cis*-reporter is probably due to endogenous TGF- $\beta$ 1 in HEK 293 cells. Transfection with wild-type *TGFBR2* resulted in a high RLA (~15), whereas transfection with the truncated mutant lacking the kinase domain,  $\delta$  cyt, gave a significantly lower RLA. Transfection with other missense mutants, L308P, S449F and R537C, also gave significantly lower RLAs, similar to that seen with transfection of  $\delta$  cyt. \* $P < 0.0001$ . **(b)** RLA of p3TP-Lux reporter in DR-26 cells (*Tgfr2*-negative) after transient transfection. Mv1Lu cells (*Tgfr2*-positive) were also used to show normal response of the p3TP-Lux reporter to TGF- $\beta$ 1. Transfection with wild-type *TGFBR2* resulted in a high RLA (~20), whereas transfection with an empty vector (pcDNA3.1(-)) or with the truncated mutant  $\delta$  cyt gave significantly lower RLAs. Transfection with other missense mutants, L308P, S449F and R537C, also gave significantly lower RLAs, similar to that seen with transfection of  $\delta$  cyt. Cotransfection of DR-26 cells with different ratios of wild-type and R537C *TGFBR2* constructs showed a serial increase of RLA in parallel with wild-type cDNA quantity, suggesting that the mutation probably did not have a dominant negative effect. \* $P < 0.0001$ .

mutation probably does not have a dominant negative effect (**Fig. 4b**). Cotransfections with wild-type protein and L308P or S449F mutants had similar results (data not shown). As we identified three classes of *TGFBR2* mutations (gene disruption, splicing and missense mutations disturbing TGF- $\beta$  signaling), loss of function probably accounts for the dominant inheritance of Marfan syndrome.

*Fbn1*-deficient mice have excessive TGF- $\beta$  activity that probably underlies their tendency to develop emphysema and could explain other manifestations of Marfan syndrome<sup>13</sup>. We previously reported that domain-specific germline mutations of *TGFBI* cause Camurati-Engelmann syndrome (OMIM 131300) and that affected individuals also usually have Marfanoid habitus (long slender extremities and vertebral deformation)<sup>14</sup>. TGF- $\beta$  regulates the extracellular matrix<sup>12,15–17</sup>. Our results provide further evidence that perturbation of TGF- $\beta$  signaling contributes to the pathogenesis of extracellular matrix disorders, but by a mechanism different from that reported in *Fbn1*-deficient mice.

Among the ten French Marfan syndrome probands examined, only four had mutations in *TGFBR2*, and these four individuals share a common clinical description: prominent aortic, skeletal and skin/integument anomalies; mild ocular anomalies (except individual MS1-IV-83, who has ectopia lentis); infrequent dural ectasia; and pulmonary abnor-

malities. These findings are not specific, however, as 100 *FBN1* mutations have been identified in Marfan syndrome probands with comparable clinical features<sup>18</sup>. Furthermore, only a small number of Marfan syndrome probands presenting with complete clinical features and not carrying a mutation in *FBN1* were screened for mutations in *TGFBR2*. Further data must be collected to assess the complete clinical spectrum associated with mutations in *TGFBR2*. Other overlapping pathologies, such as MASS syndrome (mitral valve prolapse, aortic dilatation, and skin and skeletal manifestations syndrome, OMIM 604308), isolated familial mitral valve prolapse (OMIM 157700) and autosomal dominant TAAD (OMIM 132900), should also be investigated. A locus associated with TAAD (called *TAAD2*; ref. 4) was mapped to 3p25–24, overlapping or close to the *MFS2* locus. Although no mutation was found in the ten TAAD probands that we tested, the disease is heterogeneous and further investigations are warranted before ruling out the possibility that *TGFBR2* and *TAAD2* are allelic.

In conclusion, Marfan syndrome is associated with mutations in at least two genes: *FBN1* and *TGFBR2*. The sample of families with Marfan syndrome included six French and nine Japanese probands in whom no mutation has been identified in either of these two genes. This observation could indicate that there is a higher degree of genetic heterogeneity for Marfan syndrome.

## METHODS

**Subjects and clinical evaluation:** (i) A 13-year-old Japanese boy with 46,XY,t(1;5;4)(p35;q33.2;q35),ins(3)(q11.2;p24.1p14.2) *de novo*. He underwent an operation for severe pectus excavatum at 10 years of age. He was clinically diagnosed with Marfan syndrome<sup>19</sup> because of his high arched palate, arachnodactyly (positive wrist and thumb signs), atlantoaxial subluxation, scoliosis (>20 degree), reduced extensions at the elbow, dilatation of the ascending aorta (30 mm at age 12) involving the Valsalva sinus, mitral valve prolapse, incomplete right bundle-branch block, bilateral inguinal hernia, dural ectasia by lumbo-sacral computed tomography image and increased axial length of eye globe. He presented with short stature (height of 127.0 cm (-2.9 s.d.) and weight of 21.0 kg (-2.2 s.d.)) at 12 years of age, which was evaluated as hypophyseal because stimulation with insulin or L-dopamine showed low growth hormone response (12.8 ng ml<sup>-1</sup> or 10.3 ng ml<sup>-1</sup> at the maximum growth hormone level) and blood serum IGF-I, TSH, T3 and T4 concentrations were 31.4 ng ml<sup>-1</sup> (normal range, 144–924 ng ml<sup>-1</sup>), 0.7 µU ml<sup>-1</sup> (normal range, 0.436–3.78 µU ml<sup>-1</sup>), 129 ng dl<sup>-1</sup> (normal range, 76–177 ng dl<sup>-1</sup>) and 12.9 µg dl<sup>-1</sup> (normal range, 4.8–11.2 µg dl<sup>-1</sup>), respectively. He has been treated with growth hormone since then. At the age of 13, his height was 135.2 cm (-2.8 s.d.) and weight 24.8 kg (-2.5 s.d.). PCR and direct sequencing of *FBN1* coding regions and exon-intron boundaries as described<sup>20</sup> found no mutations.

(ii) **Family MS1.** This large French family was identified after the death of a 39-year-old male family member from aortic dissection. The complete clinical features of individuals in the first part of the study were described previously<sup>3</sup>. The second part of the family study was done in the Marfan Clinic of Hôpital Ambroise Paré. Individuals at risk underwent careful physical examination, echocardiography and slit-lamp examination. Twelve new family members were evaluated and gave samples (individuals IV-40, IV-43, IV-48, V-6, V-7, V-8, V-9, V-10, V-11, V-12, V-13 and V-14). As a result, a total of 12 members (individuals III-4, III-36, III-37, III-40, III-49, III-52, IV-10, IV-44, IV-49, IV-51, IV-54 and IV-83) were diagnosed with Marfan syndrome, 14 members were found to have ambiguous status (individuals III-13, III-16, IV-30, IV-32, III-37, IV-53, IV-84, IV-86, IV-88, V-1, V-8, V-9, V-10 and V-11) and 16 unrelated spouses and 32 siblings without abnormality in any of the skeletal, ocular and cardiovascular systems (or the lung, skin-integument and central nervous system), or with only isolated minor findings in these organs or tissues, were considered unaffected. Extensive clinical data for most of these individuals were previously published<sup>3</sup>. New members from generation V with an ambiguous status carried minor skeletal features and borderline aortic root diameter. Recent clinical data are given in **Supplementary Table 1** online.

(iii) **Family MS57.** Individual II-2 presented with dolichostenomelia, pectus carinatum, arachnodactyly, mild scoliosis, spondylolisthesis, protrusio acetabulae, hyperlaxity of joints, dysmorphic face, narrow arched palate and dental crowding, striae distensae, flat cornea, aortic dilation (+8 s.d.) with mild regurgitation, mitral valve prolapse and myxoid valves, aneurysm of interatrial septum and small atrial septal defect and was diagnosed with Marfan syndrome. She died suddenly at age 18 of an unknown cause. Her brother and parents were unaffected. Her sister, individual II-1, presented with only arachnodactyly and mild pectus carinatum but no other feature of Marfan syndrome. She was considered unaffected.

(iv) **Family MS382.** Individual II-2 is a 13-year-old girl who was diagnosed with Marfan syndrome in infancy. Her father (individual I-1) died suddenly at the age of 39 of an unknown cardiovascular cause; he was tall and had hyperlaxity. Individual II-2 had pronounced skeletal symptoms of Marfan syndrome, including asymmetric pectus carinatum, arachnodactyly with positive wrist sign, dolichocephaly, severe dorso-lumbar scoliosis, hyperlaxity, joint hypermobility at ankles and knees, clear muscular hypotonia and umbilical hernia. Radiological examination showed major coxa valga and absence of dural ectasia. She presented with patent ductus arteriosus, foramen ovale, interventricular septal defect and aortic root dilation (50 mm at age 10) requiring surgery at age 12. No ocular symptom was noted, except for very slow dilation. As only two main criteria for Marfan syndrome were found, she did not fulfill the revised diagnostic criteria for Marfan syndrome. Only her mother (individual I-2) and sister (individual II-1) were available for clinical examination and showed no feature of Marfan syndrome. Blood samples were available for individuals I-2 and II-2 and were tested.

(v) **Family MS587.** Individual III-7 is a 33-year-old female who had been examined after her father's (individual II-4) sudden death at the age of 26. She had aortic dilation and mitral valve regurgitation at the age of 5, and dilation was +6 s.d. at age 31 with minimal regurgitation. She presented with a history of lung disease and pleurisy, joint hyperlaxity, narrow palate with dental crowding, scoliosis, striae distensae and mild myopia with mild astigmatism. She was diagnosed with Marfan syndrome. Family history identified two other sudden deaths: her father's brother (individual II-3) at age 22 and her father's sister (individual II-2) at age 32. Individual III-1 (age 36) showed aortic dilation, reduced upper to lower segment ratio, dolichostenomelia, pectus excavatum, narrow arched palate and scoliosis. Individual III-4 (age 30) had mild scoliosis, pectus excavatum, hyperlaxity and hypermobility of joints, high narrow palate with dental crowding, pes planus, striae distensae, and aortic dilation (+6 s.d.) with moderate aortic valve regurgitation. Individual IV-1 (age 4.5 years) presented with aortic dilation (+6 s.d.) without regurgitation, increased body length, dolichocephaly, narrow arched palate and mild scoliosis. Individuals III-1, III-4 and IV-1 were also diagnosed with Marfan syndrome. Detailed clinical information on individual IV-3, who has an ambiguous status, was not available. Blood samples were available only for individuals III-1, III-5, III-7, IV-1 and IV-3 and were tested.

(vi) **Japanese individuals with Marfan syndrome.** Ten Japanese individuals with Marfan syndrome who were shown not to carry *FBN1* mutations by PCR direct sequencing of *FBN1* coding regions and exon-intron boundaries using genomic DNA as previously described<sup>20</sup> were screened for *TGFBR2* mutations. Seven of these individuals were previously described<sup>20</sup>. All 10 individuals fit the revised criteria for Marfan syndrome<sup>19</sup>, although detailed clinical information or parental DNA was not available because materials from these individuals were treated as anonymous Marfan syndrome DNAs according to a protocol approved by the Institutional Review Board of the National Cardiovascular Center Research Institute.

(vii) **French individuals with TAAD.** Ten French individuals with TAAD were tested. All belong to families with vertical transmission of documented aortic aneurysm or dissection without risk factor for atheroma including hypertension. Inclusion criteria were ascending aortic diameter +2 s.d. above mean (ref. 21) or aortic diameter >40 mm, or operation because of dissection or dilation of the ascending aorta. Proband and family members were also systematically investigated to rule out Marfan syndrome and Ehlers-Danlos syndrome, as well as secondary aneurysm or dissection.

The French and the Japanese research protocols were approved by Comité Consultatif de Protection des Personnes dans la Recherche Biomédicale de Boulogne Billancourt Hôpital Ambroise Paré and the ethics committee of Nagasaki University, respectively. Informed consent was obtained for all individuals included in this study in agreement with the requirements of French and Japanese regulations.

**FISH analysis.** We labeled clone DNA with SpectrumGreen-11-dUTP or SpectrumOrange-11-dUTP (Vysis) by nick translation and denatured it at 76 °C for 10 min. We applied probe-hybridization mixtures (10 µl) to the chromosomes, incubated them at 37 °C for 16 h and then washed them. We carried out fluorescence photomicroscopy under a Zeiss Axioskop microscope equipped with a quad filter set with single-band excitation filters (84000, Chroma Technology). We collected and merged images using a cooled CCD camera (TEA/CCD-1317-G1, Princeton Instruments) and IPLab/MAC software (Scanalytics).

After isolating a BAC clone spanning the 3p24.1 breakpoint, we prepared a cosmid library from the BAC DNA for detailed FISH mapping. We isolated purified BAC DNA using Qiagen Midi-Prep columns (Qiagen), partially digested it with *Sau3AI* and ligated it to SuperCos1 cosmid vector according to the manufacturer's instructions (Stratagene). We extracted cosmid DNA with Qiagen Mini-Prep columns (Qiagen) and screened 182 cosmid clones by PCR.

**Mutation analysis.** We extracted genomic DNA from peripheral blood lymphocytes using standard protocols. We amplified exons 1–7 covering the *TGFBR2* coding region by PCR for direct sequencing (PCR amplification and primers sequences are available on request). PCR conditions were 35 cycles of 95 °C for 30 s, 50 °C for 30 s and 72 °C for 30 s in a 50-µl mixture, containing

1× PCR buffer with 1.5 mM MgCl<sub>2</sub>, 0.2 mM each dNTP, 1 μM each primer and 2.5 U TaqGold polymerase (Applied Biosystems). We purified PCR products with ExoSAP-IT (Amersham-Pharmacia) and sequenced both strands with BigDye Terminator chemistry version 3 by the standard protocol (Applied Biosystems). Sequencing reactions were carried out at 96 °C for 10 s, 50 °C for 5 s and 60 °C for 4 min (25 cycles) on Gene Amp PCR System 2700 or 9700 (Applied Biosystems). We purified the reaction mixture using Centri-Sep Columns (Princeton Separation) and analyzed it on the ABI Genetic Analyzer 3100 (Applied Biosystems) according to the supplier's protocols with the sequence analysis software (Applied Biosystems) and the AutoAssembler version 2.1.1 software (Applied Biosystems).

We extracted total mRNA from fibroblasts of two affected (individuals III-37 and IV-10) and one unaffected (individual III-41) members of family MS1, and a normal control person, using RNA B (Bioprobe Systems) according to the manufacturer's instructions. We treated samples with RQ1 RNase-Free DNase (Promega) and reverse-transcribed total mRNA using Superscript II RNase Reverse Transcriptase (Gibco BRL/Invitrogen). We carried out PCR analysis with a primer set in exons 5 and 7 and then sequenced the DNA as previously described. We screened and then sequenced samples from all subjects from French families by PCR on genomic DNA. All primer sequences are available on request.

**Genotyping of family MS1.** We selected microsatellite markers from public genetic databases (Généthon and CHLC) and genotyped genomic DNA as previously described<sup>2</sup>. We constructed regional haplotypes for four marker loci from tel-*D3S1609* to *D3S1619*-cen (Fig. 2; *D3S1609*, *D3S3727*, *D3S3567* and *D3S1619*). *D3S3727* is an intragenic *TGFBR2* marker. Physical mapping allowed us to determine the marker order.

**DNA constructs.** We generated wild-type *TGFBR2* cDNA (amino acids 1–567) and truncated cDNA (δ cyt; amino acids 1–222, lacking the entire kinase domain) by RT-PCR using human fetal brain BD Marathon-Ready cDNA (BD Biosciences) as a template and subcloned them into the pcDNA3.1(–) expression vector (Invitrogen). We carried out site-directed mutagenesis using the QuickChange Site-directed Mutagenesis kit (Stratagene) according to the manufacturer's protocol to generate three variant types of *TGFBR2* in pcDNA3.1(–), 923T→C, 1346C→T and 1609C→T, which were found in the families with Marfan syndrome that we studied. All variant cDNAs were verified by sequencing. Primer sequences are available on request.

**Cell culture, transfection and luciferase assay.** We grew HEK 293, Mv1Lu (a wild-type mink lung epithelial cell line) and DR-26 (a chemically mutagenized Mv1Lu cell line in which *Tgfb2* is defective)<sup>12</sup> cells in Dulbecco's modified Eagle's medium (DMEM; Sigma) containing 10% fetal bovine serum at 37 °C in a 5% CO<sub>2</sub> incubator. We transiently transfected HEK 293 cells with a *TGFBR2* construct (wild-type, δ cyt, 923T→C, 1346C→T or 1609C→T), a reporter plasmid (pTARE-Luc *cis*-reporter or pCIS-CK negative control) and a pRL-TK vector (an internal control for standardization) in Dual-Luciferase Reporter Assay System (Promega) using Transfast Transfection Reagent (Promega). The pTARE-Luc *cis*-reporter plasmid contains the basic promoter element (TATA box) and TGF-β/Activin response element (TARE). This reporter plasmid expresses firefly luciferase under control of these elements, whereas the pCIS-CK negative control plasmid contains no inducible *cis*-enhancer element to evaluate whether effects are TGF-β signaling-specific. We used p3TP-Lux containing the luciferase reporter gene under control of a portion of the plasminogen activator inhibitor type 1 (*PAI-1*) gene promoter region and three consecutive TPA response elements to evaluate extracellular matrix protein production by TGF-β signaling<sup>12</sup>. After transfection, we incubated HEK 293, Mv1Lu or DR-26 cells in DMEM for 36 h and then replaced the medium with DMEM containing 10 ng ml<sup>-1</sup> of TGF-β1. We collected cells 8 h later and assessed them for luciferase activity in quadruplicate. We measured luciferase activity using TD-20/20 Luminometer DLReady (Turner Designs Instrument). Statistical analysis was done by *post hoc* test using StatView (SAS Institute) and *P* < 0.05 was considered statistically different.

**URLs.** Généthon is available at <http://www.genethon.fr/>, and CHLC is available at <http://gai.nci.nih.gov/CHLC/>. CLUSTALW is available at <http://clustalw.genome.ad.jp/>.

**GenBank accession numbers.** *TGFBR2* cDNA, NM\_003242; *TGFBR2* coding region, NT\_022517.

*Note: Supplementary information is available on the Nature Genetics website.*

#### ACKNOWLEDGMENTS

We thank the affected individuals and their families for their participation; Y. Noguchi, K. Miyazaki and N. Yanai for technical assistance; T. Imamura and K. Miyazono for cell lines Mv1Lu and DR-26 and reporter constructs p3TP-Lux and p15P751-Luc (with permission from J. Massague); and S. Tuffery-Giraud and C. Bérout for technical and scientific discussions. This study was supported in part by CREST, Japan Science and Technology Agency, and by Université René Descartes-Paris V, Ministère de l'Éducation Nationale, de l'Enseignement Supérieur, de la Recherche et de l'Insertion Professionnelle, Fondation de France, and Faculté de Médecine Necker.

#### COMPETING INTERESTS STATEMENT

The authors declare that they have no competing financial interests.

Received 5 February; accepted 2 June 2004

Published online at <http://www.nature.com/naturegenetics/>

- Collod-Bérout, G. & Boileau, C. Marfan syndrome in the third Millennium. *Eur. J. Hum. Genet.* **10**, 673–681 (2002).
- Collod, G. *et al.* A second locus for Marfan syndrome maps to chromosome 3p24.2-p25. *Nat. Genet.* **8**, 264–268 (1994).
- Boileau, C. *et al.* Autosomal dominant Marfan-like connective-tissue disorder with aortic dilation and skeletal anomalies not linked to the fibrillin genes. *Am. J. Hum. Genet.* **53**, 46–54 (1993).
- Hasham, S. *et al.* Mapping a locus for familial thoracic aortic aneurysms and dissections (TAAD2) to 3p24-25. *Circulation* **107**, 3184–3190 (2003).
- Grady, W. *et al.* Mutational inactivation of transforming growth factor β receptor type II in microsatellite stable colon cancers. *Cancer Res.* **59**, 320–324 (1999).
- Grady, W. & Markowitz, S. Genetic and epigenetic alterations in colon cancer. *Annu. Rev. Genomics Hum. Genet.* **3**, 101–128 (2002).
- Markowitz, S. *et al.* Inactivation of the type II TGF-β receptor in colon cancer cells with microsatellite instability. *Science* **268**, 1336–1338 (1995).
- Lucke, C. *et al.* Inhibiting mutations in the transforming growth factor β type 2 receptor in recurrent human breast cancer. *Cancer Res.* **61**, 482–485 (2001).
- Parsons, R. *et al.* Microsatellite instability and mutations of the transforming growth factor β type II receptor gene in colorectal cancer. *Cancer Res.* **55**, 5548–5550 (1995).
- Tanaka, S., Mori, M., Mafune, K., Ohno, S. & Sugimachi, K. A dominant negative mutation of transforming growth factor-β receptor type II gene in microsatellite stable oesophageal carcinoma. *Br. J. Cancer* **82**, 1557–1560 (2000).
- Lu, S. *et al.* HNPCC associated with germline mutation in the TGF-β type II receptor gene. *Nat. Genet.* **19**, 17–18 (1998).
- Lu, S.-L., Kawabata, M., Imamura, T., Miyazono, K. & Yuasa, Y. Two divergent signaling pathways for TGF-β separated by a mutation of its type II receptor gene. *Biochem. Biophys. Res. Commun.* **259**, 385–390 (1999).
- Neptune, E. *et al.* Dysregulation of TGF-β activation contributes to pathogenesis in Marfan syndrome. *Nat. Genet.* **33**, 407–411 (2003).
- Kinoshita, A. *et al.* Domain-specific mutations in *TGFBI* result in Camurati-Engelmann disease. *Nat. Genet.* **26**, 19–20 (2000).
- Kissin, E.Y., Lemaire, R., Korn, J.H., & Lafyatis, R. Transforming growth factor β induces fibroblast fibrillin-1 matrix formation. *Arthritis Rheum.* **46**, 3000–3009 (2002).
- Kaartinen, V. & Warburton, D. Fibrillin controls TGF-β activation. *Nat. Genet.* **33**, 331–332 (2003).
- Annes, J., Munger, J.S. & Rifkin, D.B. Making sense of latent TGFβ activation. *J. Cell Sci.* **116**, 217–224 (2003).
- Collod-Bérout, G. *et al.* Update of the UMD-FBN1 mutation database and creation of an FBN1 polymorphism database. *Hum. Mut.* **22**, 199–208 (2003).
- De Paepe, A., Devereux, R.B., Dietz, H.C., Hennekam, R.C.M. & Pyeritz, R.E. Revised diagnostic criteria for the Marfan syndrome. *Am. J. Med. Genet.* **62**, 417–426 (1996).
- Matsukawa, R. *et al.* Eight novel mutations of the *FBN1* gene found in Japanese patients with Marfan syndrome. *Hum. Mut.* **17**, 71–72 (2001).
- Roman, M.J., Devereux, R.B., Kramer-Fox, R. & O'Loughlin, J. Two-dimensional echocardiographic aortic root dimensions in normal children and adults. *Am. J. Cardiol.* **64**, 507–512 (1989).
- Cartegni, L., Chew, S.L. & Krainer, A. Listening to silence and understanding nonsense: exonic mutations that affect splicing. *Nat. Rev. Genet.* **3**, 285–298 (2002).